International Journal of Current Research and Review
DOI: https://doi.org/10.31782/IJCRR.2024.162302

Research Article

IJCRR
Section: Healthcare

In Silico Exploration of the Potential of Drugs to Cure Obesity from the Natural Product Atlas Investigated using Computer-Aided Drug Design

Abdulaziz Alzahrani

Pharmacology & Toxicology Department, Faculty of Pharmacy, Al-Baha University, Al Baha city 65779, Saudi Arabia

ABSTRACT

Introduction: Obesity is a result of a trifecta of poor diet. Medication for obesity falls into five categories. However, due to their severe adverse effects and low efficacy, existing pharmaceutical therapies are only marginally useful. Therefore, the purpose of this research is to identify natural substances that can be used to prevent and treat obesity and associated diseases.

Methods: The 3D structure of pancreatic lipase (PDB ID: pancreatic lipase-colipase) was obtained from the protein data repository with a precision of 2.46. The file, in.pdb format, belongs to the Protein Data Bank. Natural chemicals, was obtained from PubChem. Pharmit software was used to generate the pharmacophore model. The co-crystallized structure served as the foundation for the pharmacophore model. Virtual screening is a drug discovery process that looks for structures with the best likelihood of binding to a therapeutic target. BioVIA Discovery Studio was utilized to identify two-dimensional interactions, whereas PyMOL was utilized to generate intricate receptor and ligand files. We analyze the ADMET properties of the chosen compounds using QikProp. We simulate molecular dynamics for 100 nanoseconds using Desmond software.

Results: The Natural Product Atlas database for substances was similar to the properties of the pharmacophore model. Using the PubChem data source, 33372 chemicals were assembled into a library. Sorting 1005 identified hits by their pharmacophore-fit RMSD score resulted in the selection of the top 20 compounds from pharmacophore-based virtual screening. QikProp filtered ADMET properties. Lastly, QPlogKhsa estimated the binding to human serum albumin and provided a range of 1.5 to 1.5. Two medications, NPA002198 and NPA030453, were shown to be the most effective compounds against pancreatic lipase-colipase after lead discovery. Eigenvalues (36.4-76.4% and 25.2-69.9%). The percentage of secondary structural components in pancreatic lipase-colipase-NPA030453 was calculated to be 42.44 percent, with helical and strand rates of 16.17% and 26.26%, respectively. Hydrogen bonds were the most significant receptor-ligand interactions discovered by MD. GLY_76, PHE_77, ILE_78, ASP_79, SER_152, and PHE_215 were the most important hydrogen bonding sites in the pancreatic lipase-colipase-NPA002198 complex.

Conclusion: The study found the Natural Product Atlas-approved drugs NPA002198 and NPA030453, which suppressed pancreatic lipase-colipase function. Virtual screening, docking analysis, and pharmacophore modeling was used to identify compounds with the lowest binding affinities to the target protein. We concluded that these compounds might serve as a lead chemical in the development of anti-obesity medicines. These results will benefit science by allowing researchers to develop new pharmaceuticals that can more effectively treat overweight.

Key Words: Obesity, Pancreatic lipase, Natural chemicals, Pharmacophore modeling, Compounds

INTRODUCTION

Obesity is a major and predominant component of metabolic syndrome, which can cause several serious health issues including diabetes, cholesterol, cardiovascular disease, hypertension, and cancer.[1, 2] Obesity is the accumulation of too much fat with inadequate energy expenditure, which can be harmful to health and pose a significant threat to the world's health as the number of instances rises year after year. [3, 4] Morbidity and death from obesity and all associated illnesses have dramatically increased. According to a WHO 2016 study, obesity is a chronic medical condition that affects people of all ages but is particularly prevalent in children and young adults (13%) under the age of 18. Women also have a greater prevalence rate of obesity (15%) than males (11%). [5, 6] One of the top ten health issues in western countries is obesity, which not only impacts developed countries but also emerging countries. [7-9] The FTO genes on chromosome 16 as well as the salivary and pancreas amylase genes have the

Corresponding Author:
Abdulaziz Alzahrani, Pharmacology & Toxicology Department, Faculty of Pharmacy, Al-Baha University, Al Baha city 65779, Saudi Arabia; Email: alzahraniaar@bu.edu.sa

ISSN: 2231-2196 (Print) **ISSN:** 0975-5241 (Online)

Received: 29.10.2024 **Revised:** 22.11.2024 **Accepted:** 02.12.2024 **Published:** 10.12.2024

greatest risk for obesity, according to Genome-Wide Association Studies (GWAS). These variables collectively result in annual healthcare expenditures that surpass $990 billion. [10]

The capacity to detect energy needs and produce paracrine substances to control metabolic tissues allows adipocytes to perform more than just serve as a reservoir for energy storage and consumption. When there is a sustained favorable energy balance, WAT multiplies to counteract the need for more lipid stores. Due to their constraints on expansion, these cells will eventually reach a point where they are unable to withstand additional pressure, which results in the discharge of free fatty acids into the bloodstream. Reaching this level causes adipocytes to become stressed, which in turn causes an inflammatory reaction. However, in obesity, WAT may significantly deteriorate, which encourages excessive fat buildup in other tissues and accelerates the development of renal illnesses, type 2 diabetes, and cardiovascular disease CVD.

Currently, medication for obesity falls into five categories. However, due to their severe adverse effects and low efficacy, existing pharmaceutical therapies are only marginally useful. [11] Therefore, the purpose of this research is to identify natural substances that can be used to prevent and treat obesity and associated diseases. Long been used as a significant supply of lead compounds for pharmaceutical purposes, and natural goods. The most important compounds in fruits and veggies are polyphenols [12] and their long-term intake has beneficial effects on human beings to overcome obesity, CVD, diabetes type 2, and cancer. [13-15]

Triacylglycerols, which make up dietary fat, are converted by pancreas lipase into mono glycerol and liberated fatty acids, which are readily absorbed by living things. [16] This pancreatic-secreted enzyme breaks down 50–70% of ingested lipids. Therefore, we can suppress pancreatic lipase to prevent fat from being absorbed into the gastrointestinal system and to manage obesity. This pancreatic-secreted enzyme breaks down 50–70% of ingested lipids. Therefore, we can suppress pancreatic lipase to prevent fat from being absorbed into the gastrointestinal system and regulate obesity. We have used natural substances as pancreatic lipase inhibitors. Many different enzymes, including lipoxygenase, cyclooxygenase, 3-kinase phosphoinositide, and xanthine oxidase, are thought to be actively inhibited by natural products. Natural compounds also play a number of defensive functions in the human body. [17, 18]

The primary goal of pancreatic lipase inhibition is to decrease gastrointestinal fat intake by stopping its action. The fecal pathway is used to expel the triglycerides that were not ingested. Additionally, pancreatic lipase inhibitors may not have the adverse effects that are frequently connected to other important antiobesity medications. [19, 20] In the current effort, we used a collection from The Natural Product Atlas and used docking tools to screen them. One target, many ligands is a computational technique called virtual screening that is used to evaluate a large collection of molecules. Molecules that passed the screening process were exposed to an ADME prediction; QikProp is used to ascertain the ADME characteristics. A select few substances with anti-obesity activity were advanced to docking experiments to investigate the molecular contacts between the substance and lipase. A Molecular Dynamic Simulation was performed to confirm the target enzyme-ligand complex's stability. [21, 22]

MATERIALS AND METHODS

Target protein retrieval, optimization and Minimization

The 3D structure of pancreatic lipase (PDB pancreatic lipase-colipase) was obtained from the protein data repository with a precision of 2.46. The file, in.pdb format, belongs to the Protein Data Bank. Co-crystallized water atoms in the active site were deleted beyond 5.00 Angstrom; the accuracy of docking can be impacted by the removal of water molecules. Protein Data Bank offers web-based information centers and a downloadable data library including 3D structural data and associated information for macromolecules like proteins, DNA, and RNA. [16, 23, 24] The 3D structure of pancreatic lipase (PDB ID: pancreatic lipase-colipase) was obtained from the protein data repository with a precision of 2.46. Co-crystallized water atoms in the active site were deleted beyond 5.00 Angstrom; the accuracy of docking can be impacted by the removal of water molecules. Protein Data Bank offers web-based information centers and a downloadable data library including 3D structural data and associated information for macromolecules like proteins, DNA, and RNA.[25-28]

Database Preparation

The Natural Products Atlas, an extensive database of natural chemicals, was obtained from PubChem. The Lipinski criterion was utilized to choose molecules with drug-like behavior. In all, 32552 compounds were found. The medications were downloaded as SD files. Subsequently, the medications were converted to the format for Pharmit virtual screening. [29, 30]

Pharmacophore Modeling and Virtual Screening

Pharmit software was used to generate the pharmacophore model. The co-crystallized structure served as the foundation for the pharmacophore model. Virtual screening is a drug discovery process that looks for structures with the best likelihood of binding to a therapeutic target based on unique characteristics and descriptors among libraries of compounds. Pharmit software was used to aid with this, and the database was used. [30]

Molecular Docking, ADMET Analysis and Lead Identification

After classifying the highest-scoring hits according to their pharmacophore-fit RMSD score for pancreatic lipase-colipase, the top 20 compounds from pharmacophore-based virtual screening were selected. Employing Vina AutoDock. These top 20 substances' binding affinities and protein-ligand interactions were examined after they were docked with receptors. BioVIA Discovery Studio was utilized to identify two-dimensional interactions, whereas PyMOL was utilized to generate intricate receptor and ligand files. [31-33] We analyze the ADMET properties of the chosen compounds using QikProp. The processes of absorption, diffusion, metabolism, and excretion provide information on the quantity and energy of the drug. We can enhance a powerful drug's performance using these elements. These show how well the substance works as a medication.[34] The most successful inhibitors were identified through the use of the following methods: toxicology examination research, including Molecular Weight (MW), Hydrogen Bond Donner (HBD), Hydrogen Bond Acceptor (HBA), rings, Polar Surface Area (PSA), rotatable bonds, Blood-Brain Barrier, and Ames Toxicity; docking score; RMSD values; protein-ligand interactions; lead and drug likeness analysis; and lead likeness and drug likeness analysis. As putative anti-aggregation inhibitors, compounds with the lowest binding affinities, lowest RMSD values, maximum lead likeness, and best interactions were selected.

Molecular Dynamics Simulation

We simulate molecular dynamics for 100 nanoseconds using Desmond software. Docking findings provided the simulation's input complicated. Protein and ligand binding was analyzed in both stiff and static modes using docking. Molecular dynamics simulation forecasts the energies and interactions between proteins and ligands over the simulation period in a physiological setting.[35-38]. The protein-ligand combination was preprocessed, optimized, and minimized using the Protein Preparation Wizard of Maestro. After that, the complex was ready for simulation using System Builder. The solvent model we utilized was TIP3P (Intermolecular Interaction Potential 3 Points Transferable), with an orthorhombic grid, a temperature of 310 K, a pressure of 1 atm, and an OPLS_2005 force field. In order to replicate the physiological milieu, we add 0.15 M sodium chloride, and we also add ions to neutralize the system. In order to ensure that the ions do not interfere with the protein-ligand interactions in simulation, we build an exclusion zone for the ligand when we add ions, measuring 20 Angstroms. We saved the trajectories for each 100 ps interval during the 100 ns simulation. Using the R "Bio3D" package, principal component analysis (PCA) and dynamic cross-correlation matrix (DCCM) were examined. [39, 40]

RESULTS

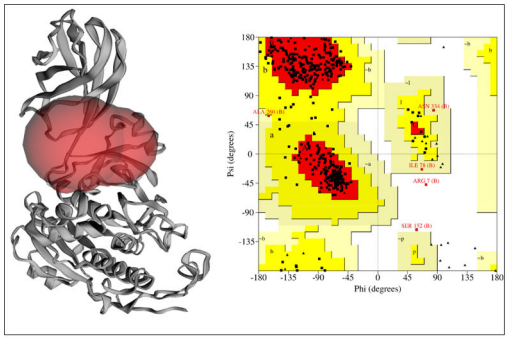

Figure 1: Different regions of the protein structure are displayed in the Ramachandran plot of the 3D structure of a protein that was taken from PDB pancreatic lipase-colipase (which has a predicted active site).

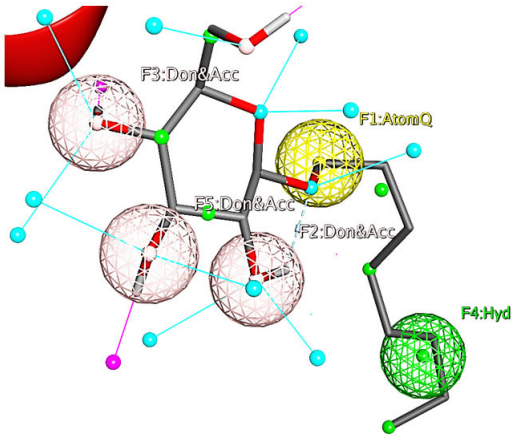

Figure 2: Selective ligand fit based on pharmacophore theory and ligand-based pharmacophore (pancreatic lipase-colipase)

Table 1: Table displaying the selected compounds structure with name, binding affinity, and pharmacophore score and ADMET properties.

MoleculePubChem ID	mol_MW	donorHB	accptHB	QPlogPo/w	QPlogHERG	QPPCaco	QPlogBB	QPlogKhsa	Pharmacophore RMSD	Binding Affinity
NPA030453	364.227	0	9.75	0.152	-5.776	77.837	-1.866	-1.132	0.48383	-8.0
NPA028586	448.218	0	23	-7.278	-5.392	0.213	-4.51	-4.137	0.4639	-7.1
NPA029087	784.474	0	22	-0.165	-7.252	1.973	-4.496	-1.333	0.4667	-6.8
NPA002198	276.161	0	10.5	-1.862	-5.8	10.209	-2.717	-1.229	0.4511	-7.7
NPA033131	476.268	0	19.25	-3.95	-5.383	46.709	-1.912	-3.138	0.4141	-8.8

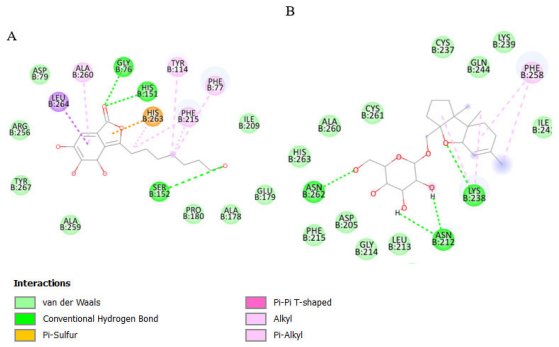

Figure 3: The kinds of contacts and interacting residues together with their distances are displayed in the interactions between NPA002198 (A) and NPA030453 (B) with the pancreatic lipase-colipase protein target.

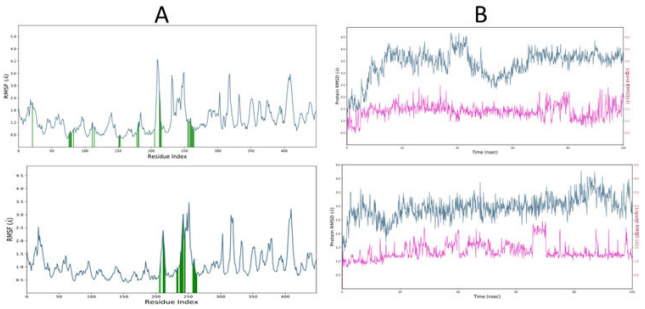

Figure 4: A. RMSF (pancreatic lipase-colipase-NPA002198; & pancreatic lipase-colipase-NPA030453).B. RMSD of the ligand pancreatic lipase-colipase complexed with (pancreatic lipase-colipase-NPA030453) &NPA002198 over time, as well as the target proteins' carbon alpha atoms. The left Y-axis depicts how the RMSD of proteins and ligands varies with time. (The red color denotes ligand RMSD, whereas the blue hue indicates protein RMSD.)

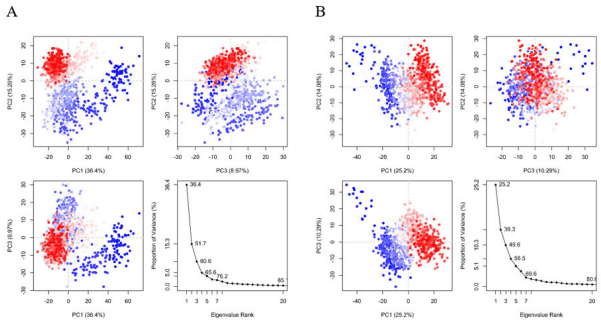

Figure 5: Eigenvalue from Principal Component Analysis shown versus variance percent. A) The pancreatic lipase-colipase-NPA002198 complex is divided into three unique sections, each depicting a different area. PC1, PC2, and PC3 varieties account for 36.4%, 15.26%, and 8.97%, respectively. B) The complicated modifications in PC1, PC2, and PC3 in pancreatic lipase-colipase-NPA030453 total 25.2%, 14.08%, and 10.29%, respectively.

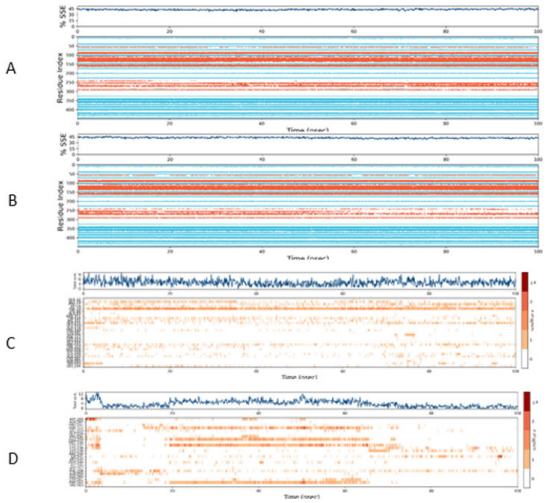

Figure 6: Elements of Protein Secondary Structure, such strands and helices, are arranged residue-by-residue in protein structures that are complexed with ligand molecules. Alpha helices are represented by red columns, and beta strands by blue columns. (Pancreatic lipase-colipase-NPA002198 for A and pancreatic lipase-colipase-NPA030453 for B). The whole simulation involves interactions between proteins and ligands. (NPA030453, NPA002198) C&D.

DISCUSSION

With the help of the Protein Data Bank, the 3D structure of the receptor was found. The overall weight of the pancreatic lipase-colipase structure is 61.65 kDa. It has stoichiometry for Hetero 2-mer-A1B1 and asymmetric-C1 global symmetry. The protein structure is shown in Figure 1 following loop optimization, refinement, minimization, and the corresponding Ramachandran plot. The overall quality of the structure was 98 percent, with observations that were highly favored. Proline is represented as squares in the figure, and glycine by triangles, with all other residues shown as circles. "Favoured" places are the orange areas, "allowed" areas are the yellow regions, and "disallowed" areas are the white areas.

The co-crystallized molecule was chosen for the Pharmit pharmacophore model creation. Combined pharmacophoric qualities based on complementary traits are displayed in Fig. 2. Common pharmacophoric features include hydrophobic centroids, cations, anions, aromatic rings, hydrogen bond acceptors or donors. These pharmacophoric sites might be projecting spots inside the receptor or they can be found on the ligand itself. F1 denotes the atomQ functional group for the protein target, whereas F2, F3, and F5 stand for the donor functional group and hydrogen-bond acceptors, respectively. Hydrophobic function group is represented by F5. Following pharmacophore modeling, Pharmit was used to virtually filter the Natural Product Atlas database for substances with

properties similar to the pharmacophore model. Using the PubChem data source, 33372 chemicals were assembled into a library. Sorting 1005 identified hits by their pharmacophore-fit RMSD score resulted in the selection of the top 20 compounds from pharmacophore-based virtual screening. Table 1 lists the binding affinity, pharmacophore score, and two-dimensional structure of the top five drugs.

Mol_MW represents the molecular weights of the compounds in Table 1, which are suggested to be between 130.0 and 725.0. AccptHB is the expected number of hydrogen bonds that are accepted or absorbed by water molecules in an aqueous medium, whereas donorHB is the estimated number of hydrogen bonds that the solute would provide to water molecules. The proposed values for donorHB and AccptHB are non-integer averages ranging from 0.0 to 6.0 and 2.0 to 20.0.QPlogPo/w represents the expected octanol/water partition coefficient, which varies from -2.0 to 6.5. Determine the IC50 value of HERG K+ channel inhibition using QPlogHER. Issues that do not rank higher than five. The apparent permeability of Caco-2 cells is calculated by QPPCaco in nm/sec. The gut-blood barrier may be modeled using Caco2 cells. QikProp uses criteria ranging from <25 (poor) to >500 (great) to estimate passive transport. Blood brain barrier permeability is predicted by QPlogBB, whereas oral medications with unsuitable ADMET properties are filtered by QikProp. Lastly, QPlogKhsa Estimate the binding to human serum albumin and provide a range of 1.5 to 1.5. Two medications, NPA002198 and NPA030453, were shown to be the most effective compounds against pancreatic lipase-colipase after lead discovery. The best two-dimensional interactions are shown in Figure 3. The attributes of the best ones are displayed in Table 1.

Target proteins were simulated using MD for 100 nanoseconds using the best compounds, and then the computer paths were inspected. Different kinds of analysis, including protein-ligand interactions, RMSD, and RMSF, were determined as part of MD trajectory analysis.

The evolution of the RMSD values for carbon alpha atoms in proteins linked to ligands is seen in Figure 4. The proteins in the complex (NPA002198-pancreatic lipase-colipase) stabilized at 10 ns, according to the RMSD curve. After then, RMSD values fluctuate during the simulation within 1.0 Angstrom, which is perfectly typical and acceptable. Little structural variation is produced by the protein RMSD structure, which is only marginally increasing at 60 ns. The trial showed that the structure was strong overall. The ligand maintained its equilibrium for the course of the experiment. Occasionally, there were sudden increases or decreases in the RMSD readings. The fact that the ligand RMSD did not change once equilibrium was attained indicates that a ligand mode transition was the cause of this.

The evolution of the RMSD values for carbon alpha atoms in proteins coupled to ligands is seen in Figure 4. The proteins in the complex (pancreatic lipase-colipase-NPA030453) stabilized 20 ns after the workout started, according to the RMSD graph. For the rest of the test, up to 80 ns, the RMSD measurements varied within 1.0 Angstrom before climbing consistently. The pancreatic lipase-colipase RMSD's structure seldom changes between 80 and 90 ns, which leads to minimal structural variance and stability. After that, it resumed being steady. The ligand reached equilibrium at 10 ns and stayed there for the duration of the experiment. Over the course of the trial, the ligand RMSD stayed constant.

Protein dynamics are described by Principal Component Analysis (PCA). Observing collective trajectory movements in MD simulations is an effective strategy. Figure 6 shows a graph of eigenvalues (protein) vs eigenvector index. The eigenvalues indicate the oscillations of hyperspace eigenvector. Larger eigenvectors control the overall mobility of proteins in simulations. In our systems, the top five eigenvectors exhibited dominating movements and had higher eigenvalues than the other eigenvectors, which had lower eigenvalues (36.4-76.4% and 25.2-69.9%). More over half of the changes were attributable to the first three plotted PCs (PCs 1, 2, and 3). [41] The PC1 clusters showed the most variability (36.4%) and (25.2%), followed by the PC2 clusters (15.26%) and (14.08%), and the PC3 clusters (8.97%) and (10.29%), respectively, in the Fig. 5 plots for pancreatic lipase-colipase-NPA002198 and pancreatic lipase-colipase-NPA030453. PC3 is predicted to have the most stable protein-ligand interactions due to its low variability, which also gives it a more compact structure than PC1 and PC2. All groups' conformational variations were shown by simple grouping in the PC subspace, with blue denoting the most mobility, white suggesting intermediate movement, and red denoting less flexibility.

The target protein's RMSF value when complexed with ligand is displayed in Figure 4. The N-terminus and C-terminus, together with lops and coils, have larger RMSF because of free ends, according to MD simulation data. Alpha-helical and beta-sheet residues are less common in RMSF compared to loop and coil residues. The residues in contact with the ligand have a lower RMSF because the residues in helixes and sheets are less flexible and more rigid (Figure 6). During the modeling procedure, filaments and helices were recognized as secondary structural elements (SSE). The graph below shows the distribution of secondary structure components over the simulation time period, organized by residue. The beta strand and alpha helix percentages in pancreatic lipase-colipase-NPA002198 were calculated to be 26.00 and 16.64, respectively, for a total secondary structural element proportion of 42.64. The percentage of secondary structural components in pancreatic lipase-colipase-NPA030453 was calculated to be 42.44 percent, with helical and strand rates of 16.17% and 26.26%, respectively. Figure 9 shows that

hydrogen bonds are the most significant receptor-ligand interactions discovered by MD. GLY_76, PHE_77, ILE_78, ASP_79, SER_152, and PHE_215 are the most important hydrogen bonding sites in the pancreatic lipase-colipase-NPA002198 complex. The most important hydrogen bonds in pancreatic lipase-colipase-NPA030453 are ASN_212, GLU_233, CYS_237, ILE_241, PHE_258, and ASN_263. During the simulation, ligand-containing protein was seen. The graph depicts the total number of interactions and contacts between proteins and ligands over time, which include hydrogen bonds, ionic, hydrophobic, and water bridges. Compared to NPA030453, NPA002198 medication demonstrated greater stability with the protein target in terms of RMSD stability, PCA, and number of contacts during simulation.

CONCLUSION

Several multidisciplinary techniques have piqued scientific attention as a means of accelerating and lowering the cost of pharmaceutical research. The primary purpose of this effort was to identify target proteins, followed by the selection of a lead lipase inhibitor. We look for the Natural Product Atlas-approved drugs NPA002198 and NPA030453, which suppress pancreatic lipase-colipase function. Virtual screening, docking analysis, and pharmacophore modeling were used to identify compounds with the lowest binding affinities to the target protein. We concluded that these compounds might serve as a lead chemical in the development of anti-obesity medicines. These results will benefit science by allowing researchers to develop new pharmaceuticals that can more effectively treat overweight.

ACKNOWLEDGMENT

Author acknowledge the immense help received from the scholars whose articles are cited and included in references of this manuscript. The authors are also grateful to "Department of pharmaceutical chemistry member staff"

Authors' Contribution

Single author, Alzahrani: contributed new finding and analytical tools, performed data analysis, Wrote the manuscript, Review and editing of the manuscript.

Source of Funding:

The author received no financial support for the research, authorship, and/or publication of this article.

Conflict of Interest

The author declared no potential conflicts of interest with respect to the research, authorship, and/or publication of this article.

Ethical approval:

Not applicable an ethical approval for kind this study.

Data availability statement

All data used to support the findings of this study are available from the corresponding author upon request.

REFERENCES

1. Lovren F, Teoh H, Verma S. Obesity and atherosclerosis: mechanistic insights. Can j Cardiol[Internet].2015;31(2):177–83.Availablefrom: https://www.ncbi.nlm.nih.gov/pubmed/25661552.
2. Rahmouni K. Obesity-Associated Hypertension. Hypertension. 2014 Aug;64(2):215–21.
3. Mittendorfer B, Peterson LR. Cardiovascular consequences of obesity and targets for treatment. Drug Discov. Today: Therapeutic Strategies. 2008 Mar;5(1):53–61.
4. Gersh BJ. National, regional, and global trends in body-mass index since 1980: systematic analysis of health examination surveys and epidemiological studies with 960 country-years and 9·1 million participants. Yearbook of Cardiology. 2012 Jan;2012:252–4.
5. Kim KB, Shin YA. Obese and Overweight Males. J Obes Metab Syndr. 2020 Mar 9;
6. WHO | Global Health Observatory (GHO) data [Internet]. apps.who.int. Available from: https://apps.who.int/gho/data/motd.html
7. Evans RM, Barish GD, Wang YX. PPARs and the complex journey to obesity. Nat. Med. 2004 Mar 31;10(4):355–61
8. Bhurosy T, Jeewon R. Overweight and Obesity Epidemic in Developing Countries: A Problem with Diet, Physical Activity, or Socioeconomic Status? Sci. World J. [Internet]. 2014;2014:1–7. Available from: https://www.ncbi.nlm.nih.gov/pmc/articles/PMC4212551/
9. Fall T, Ingelsson E. Genome-wide association studies of obesity and metabolic syndrome. Mol. Cell. Endocrinol. 2014 Jan;382(1):740–57.
10. Loos RJF, Yeo GSH. The genetics of obesity: from discovery to biology. Nat. Rev. Genet [Internet]. 2021 Sep 23;23(23):1–14. Available from: https://www.nature.com/articles/s41576-021-00414-z
11. Oh TJ. The Role of Anti-Obesity Medication in Prevention of Diabetes and Its Complications. J. Obes. Metab. Syndr. 2019 Sep 30;28(3):158–66.
12. Manach C, Scalbert A, Morand C, Rémésy C, Jiménez L. Polyphenols: food sources and bioavailability. Am. J. Clin. Nutr. 2004 May 1;79(5):727–47.
13. Godos J, Vitale M, Micek A, Ray S, Martini D, Del Rio D, et al. Dietary Polyphenol Intake, Blood Pressure, and Hypertension: A Systematic Review and Meta-Analysis of Observational Studies. Antioxidants (Basel, Switzerland) [Internet]. 2019 May 31 [cited 2020 Jul 18];8(6). Available from: https://pubmed.ncbi.nlm.nih.gov/31159186/
14. Konstantinidi M, Koutelidakis AE. Functional Foods and Bioactive Compounds: A Review of Its Possible Role on Weight Management and Obesity's Metabolic Consequences. J. Med [Internet]. 2019 Sep 9;6(3). Available from: https://www.ncbi.nlm.nih.gov/pmc/articles/PMC6789755/
15. Wang T, Li Q, Bi K. Bioactive flavonoids in medicinal plants: Structure, activity and biological fate. Asian J Pharm Sci. 2018 Jan 1;13(1):12–23.

16. Bourne Y, Martinez C, Kerfelec B, Lombardo D, Chapus C, Cambillau C. Horse Pancreatic Lipase. J Mol Biol. 1994 May;238(5):709–32
17. Lee EM, Lee SS, Chung BY, Cho JY, Lee IC, Ahn SR, et al. Pancreatic Lipase Inhibition by C-Glycosidic Flavones Isolated from Eremochloa ophiuroides. Molecules. 2010 Nov 16;15(11):8251–9.
18. Birari RB, Bhutani KK. Pancreatic lipase inhibitors from natural sources: unexplored potential. Drug Discov. Today. 2007 Oct;12(19-20):879–89.
19. Heck AM, Yanovski JA, Calis KA. Orlistat, a new lipase inhibitor for the management of obesity. J. Pharmacother [Internet]. 2000 [cited 2019 Nov 5];20(3):270–9. Available from: https://www.ncbi.nlm.nih.gov/pubmed/10730683
20. Huo PC, Hu Q, Shu S, Zhou QH, He RJ, Hou J, et al. Design, synthesis and biological evaluation of novel chalcone-like compounds as potent and reversible pancreatic lipase inhibitors. Bioorg. Med. Chem.. 2021 Jan;29:115853.
21. Madhavi Sastry G, Adzhigirey M, Day T, Annabhimoju R, Sherman W. Protein and ligand preparation: parameters, protocols, and influence on virtual screening enrichments. J. Comput. Aided Mol. Des [Internet]. 2013 Mar [cited 2019 Jun 26];27(3):221–34. Available from: https://link.springer.com/article/10.1007%2Fs10822-013-9644-8
22. Iqbal MN, Rasheed MA, Awais M, Chammam W, Kanwal S, Khan SU, et al. BMT: Bioinformatics mini toolbox for comprehensive DNA and protein analysis. Genomics [Internet]. 2020 Nov 1 [cited 2022 Nov 7];112(6):4561–6. Available from: https://www.sciencedirect.com/science/article/pii/S0888754320309782
23. Berman HM. The Protein Data Bank. Nucleic Acids Res. 2000 Jan 1;28(1):235–42.
24. Veeramachaneni GK, kodamala KR, Chalasani LM, J S B, Talluri VR. High-throughput virtual screening with e-pharmacophore and molecular simulations study in the designing of pancreatic lipase inhibitors. Drug Des. Devel. Ther. 2015 Aug;4397.
25. Eswar N, Webb B, Marti-Renom MA, Madhusudhan MS, Eramian D, Shen M, et al. Comparative Protein Structure Modeling Using MODELLER. Curr Protoc Protein Sci. 2007 Nov;50(1):2.9.1–31.
26. Guex N, Peitsch MC. SWISS-MODEL and the Swiss-Pdb Viewer: An environment for comparative protein modeling. Electrophoresis. 1997;18(15):2714–23
27. Ho BK, Brasseur R. The Ramachandran plots of glycine and pre-proline. BMC Struct. Biol [Internet]. 2005;5(1):14. Available from: https://bmcstructbiol.biomedcentral.com/articles/10.1186/1472-6807-5-14
28. Tian W, Chen C, Liang J. CASTp 3.0: Computed Atlas of Surface Topography of Proteins and Beyond. Biophys J. 2018 Feb;114(3):50a
29. van Santen JA, Jacob G, Singh AL, Aniebok V, Balunas MJ, Bunsko D, et al. The Natural Products Atlas: An Open Access Knowledge Base for Microbial Natural Products Discovery. ACS Cent. Sci. 2019 Nov 14;5(11):1824–33
30. Sunseri J, Koes DR. Pharmit: interactive exploration of chemical space. Nucleic Acids Res. 2016 Apr 19;44(W1):W442–8.
31. Trott O, Olson AJ. AutoDock Vina: Improving the Speed and Accuracy of Docking with a New Scoring function, Efficient optimization, and Multithreading. J Comput Chem. 2009;31(2).
32. Mura C, McCrimmon CM, Vertrees J, Sawaya MR. An Introduction to Biomolecular Graphics. PLoS Comput. Biol [Internet]. 2010 Aug 26;6(8):e1000918. Available from: https://www.ncbi.nlm.nih.gov/pmc/articles/PMC2928806/
33. Systèmes D. Free Download: BIOVIA Discovery Studio Visualizer [Internet]. Dassault Systèmes. 2020. Available from: https://discover.3ds.com/discovery-studio-visualizer-download
34. Cheng F, Li W, Zhou Y, Shen J, Wu Z, Liu G, et al. admetSAR: A Comprehensive Source and Free Tool for Assessment of Chemical ADMET Properties. J Chem Inf Model. 2012 Nov;52(11):3099–105.
35. Bowers KJ, Sacerdoti FD, Salmon JK, Shan Y, Shaw DE, Chow E, et al. Molecular dynamics---Scalable algorithms for molecular dynamics simulations on commodity clusters. Proceedings of the 2006 ACM/IEEE conference on Supercomputing - SC '06. 2006;
36. Ferreira L, dos Santos R, Oliva G, Andricopulo A. Molecular Docking and Structure-Based Drug Design Strategies. Molecules. 2015 Jul 22;20(7):13384–421.
37. Hildebrand PW, Rose AS, Tiemann JKS. Bringing Molecular Dynamics Simulation Data into View. Trends Biochem. Sci [Internet]. 2019 Nov 1 [cited 2023 Feb 13];44(11):902–13. Available from: https://www.sciencedirect.com/science/article/pii/S0968000419301379
38. Rasheed MA, Iqbal MN, Saddick S, Ali I, Khan FS, Kanwal S, et al. Identification of Lead Compounds against Scm (fms10) in Enterococcus faecium Using Computer Aided Drug Designing. Life. 2021 Jan 21;11(2):77.
39. Shivakumar D, Williams J, Wu Y, Damm W, Shelley J, Sherman W. Prediction of Absolute Solvation Free Energies using Molecular Dynamics Free Energy Perturbation and the OPLS Force Field. J. Chem. Theory Comput. 2010 Apr 14;6(5):1509–19.
40. Grant BJ, Lars Skjærven, Yao X. The Bio3D packages for structural bioinformatics. 2020 Aug 17;30(1):20–30
41. David CC, Jacobs DJ. Principal Component Analysis: A Method for Determining the Essential Dynamics of Proteins. Protein Dynamics. 2013 Sep 3;193–226.